

Systematics of the positive muon Knight shift in simple metals

M. Manninen

Swiss Institute for Nuclear Research, CH-5234 Villigen, Switzerland

(Received 14 June 1982)

The Knight shift of the positive muon in simple metals is calculated self-consistently including both the contact spin-density term and the diamagnetic shielding. The lattice potential is described in the spherical-solid model. A systematic behavior as a function of r_s and the valency of the host metal is found in good agreement with the experimental results. The effects of the lattice relaxation and the muon zero-point motion are estimated. The Knight shifts for muons trapped at lattice vacancies are predicted.

I. INTRODUCTION

The precession frequency of positive muons has been measured practically in all nontransition metals.¹⁻³ Most of the theoretical work has been based on the jellium approximation where the metal is described by a homogeneous electron gas.⁴⁻⁶ The experimental Knight shifts, however, do not show the simple dependence only on the electron-density parameter r_s , predicted by the jellium model. Molecular-cluster calculations⁷⁻⁹ have given a better agreement with the experimental results in some single cases, but no systematic study has been made. Also the band-structure techniques have not been applied to simple metals, although they provide good results in magnetic materials.^{10,11}

The jellium model gives a good description for the positron annihilation in simple metals,¹² indicating that the total charge density at the impurity site is well described. Also, when applied to the nuclear Knight shifts in simple metals^{13,14} the jellium model gives good agreement with experimental results. The discrepancy of the experimental muon Knight shift from the jellium results shows that the spin density, as opposed to the charge density, is very sensitive to the actual lattice potential. This can be included in the jellium model with the use of perturbation theory or by applying the spherical-solid model.^{15,16} In an earlier paper¹⁶ we applied the spherical-solid model for calculating the muon Knight shift, electric field gradient, and energetics of muon in Al, Na, and Cu. In this paper we do a more comprehensive calculation of muon Knight shifts in simple metals. The results show that the lattice pseudopotentials affect drastically the Knight shift, and the inclusion of them in the spherical approximation brings the jellium results close to the experimental ones. It is shown that for a given valency of the host the muon Knight shift is nearly a smooth function of r_s and shows a systematic

behavior, which is in good agreement with the experimental results.

Owing to the very light mass, the amplitude of the muon zero-point motion is an appreciable amount of the lattice constant, and thus the muon scans a region where the effective lattice potential varies markedly. In the ferromagnetic materials this has a large effect (even more than 50%) on the measured hyperfine field.¹⁷⁻¹⁹ In simple metals where the lattice potential is nonmagnetic the effect of the zero-point motion turns out to be much smaller ($\lesssim 10\%$). Similarly, the estimated effect of the lattice relaxation around the muon is smaller.

II. THEORETICAL MODEL

In the jellium model the electronic structure of an impurity is calculated by embedding the impurity nucleus into a homogeneous (polarized) electron gas and calculating the screening self-consistently. In the spherical-solid model the compensating positive background charge of the jellium model is replaced by the unscreened pseudopotentials spherically averaged around the impurity site. The resulting spherical-solid potential $V_{ss}(r)$ approaches the exact lattice pseudopotential in the immediate vicinity of the impurity, whereas it becomes a constant far away from the impurity.¹⁶ The screening of this potential and the impurity nucleus is calculated self-consistently using the density functional Kohn-Sham method (for computational details see Refs. 16 and 20 and references therein).

For spherical symmetry the Knight shift (the ratio between the hyperfine field and the external magnetic field) consists of two terms,

$$K = K_c + K_d, \quad (1)$$

where K_c comes from the contact interaction, and K_d from the diamagnetic shielding. The contact term can be written as

$$K_c = -\frac{8\pi}{3}\mu_B[n^\uparrow(\vec{r}_\mu) - n^\downarrow(\vec{r}_\mu)]/H_{\text{ext}}, \quad (2)$$

where $n^\uparrow(\vec{r}_\mu)$ and $n^\downarrow(\vec{r}_\mu)$ are the spin-up and spin-down densities at the muon site, μ_B the Bohr magneton, and H_{ext} the external magnetic field. Far away from the impurity where the potential is constant, H_{ext} produces a constant polarization $n_0^\uparrow - n_0^\downarrow$ for the homogeneous electron gas. With the help of the spin susceptibility of the homogeneous electron gas χ_s , one can write

$$K_c = \frac{8\pi}{3}\chi_s\rho_s(\vec{r}_\mu), \quad (3)$$

where $\rho_s(\vec{r})$ is the spin-density enhancement defined as

$$\rho_s(\vec{r}) = [n^\uparrow(\vec{r}) - n^\downarrow(\vec{r})]/(n_0^\uparrow - n_0^\downarrow). \quad (4)$$

The lattice potential affects the Knight shift in two ways: (i) It makes the electron and spin densities of the host metal inhomogeneous, and (ii) it

$$K_d = -\frac{1}{3c^2} \int_0^\infty dr 4\pi r \Delta n(r) + \frac{2k_F}{3\pi^2} \int_0^\infty dr \frac{1}{r} \sum_l l(l+1)(2l+1)[R_{lk_F}^2(r) - j_l^2(k_F r)], \quad (6)$$

where c is the velocity of light, $\Delta n(r)$ the induced electron density around the muon, $R_{lk_F}(r)$ the radial wave function at the Fermi energy, and $j_l(k_F r)$ the spherical Bessel function. This formula is directly applicable also for the spherical-solid model.

The effect of the muon zero-point motion can be estimated by calculating the Knight shift adiabatically at different lattice sites and taking an average over the muon distribution,

$$K_{\text{av}} = \int d\vec{r} K(\vec{r})P_\mu(\vec{r}), \quad (7)$$

where $P_\mu(\vec{r})$ is the probability that the muon is at point \vec{r} . $K(\vec{r})$ is the Knight shift calculated by embedding the muon at point \vec{r} and taking the spherical average of the lattice potential around that point.

In the spherical-solid model the host metal is described by the electron-density parameter r_s , valency Z , lattice structure, and the pseudopotential. For the pseudopotential we used the simple Ashcroft empty-core potential²¹ with commonly used core radii [from Ref. 21 except for Cu,²² Be,²³ Cd,²³ Ca,²³ Sr,²⁴ and Ba (Ref. 24)].

III. RESULTS AND DISCUSSION

A. Knight shift at an interstitial muon

The muon was first assumed to be a fixed point charge at the center of the interstitial site. The

changes the spin susceptibility from the homogeneous electron-gas value. In the spherical-solid model both these effects are approximately included around the impurity. The spherical-solid potential (without the impurity) not only produces an inhomogeneous spin density around the impurity, but also changes locally the total spin density so that

$$\int d\vec{r} [\rho_s(\vec{r}) - 1] \neq 0. \quad (5)$$

This nonzero induced moment is an indication of a local change in the spin susceptibility due to the spherical-solid potential. Thus in the above formulation all the lattice effects are included in $\rho_s(\vec{r})$. The susceptibility in Eq. (3) is for a homogeneous (interacting) electron gas¹⁶ and the use of, e.g., an experimental spin susceptibility would not be consistent.

The second contribution to the Knight shift is the diamagnetic shielding. For the jellium model Zaremba and Zobin⁶ have derived a formula (in a.u.)

Knight shift including both contact and diamagnetic contributions was calculated in the jellium model and in the spherical-solid model for both tetrahedral and octahedral interstitial sites. fcc lattice structure was taken for hcp metals. The results for mono- and divalent metals are shown in Figs. 1 and 2, respectively. The jellium model, even with the diamagnetic contribution, gives too large values for all simple metals. The spherical-solid model systematically improves the results and gives generally a very good agreement with the experimental results,³ also shown in the figures. The only exceptions are Li and Be where the theory predicts much too large Knight shifts. In these metals the measured spin susceptibility differs very much from the electron-gas value, and thus it is not surprising that the spherical-solid model based on a simple local pseudopotential cannot describe correctly the complicated magnetic properties of Li and Be.

In alkali metals the difference between different lattice sites is very small, but it becomes larger in divalent metals where the pseudopotential is stronger. Also, the difference between the octahedral and tetrahedral sites is larger in the fcc structures than in the open bcc structures. For Al ($Z=3$) the spherical-solid model gives for the octahedral site 85 ppm, whereas the experimental result is 80 ± 4 ppm. For Pb ($Z=4$) the theory gives 230 ppm, whereas the experimental result is only 105 ppm.

The sensitivity of the Knight shift on the pseudo-

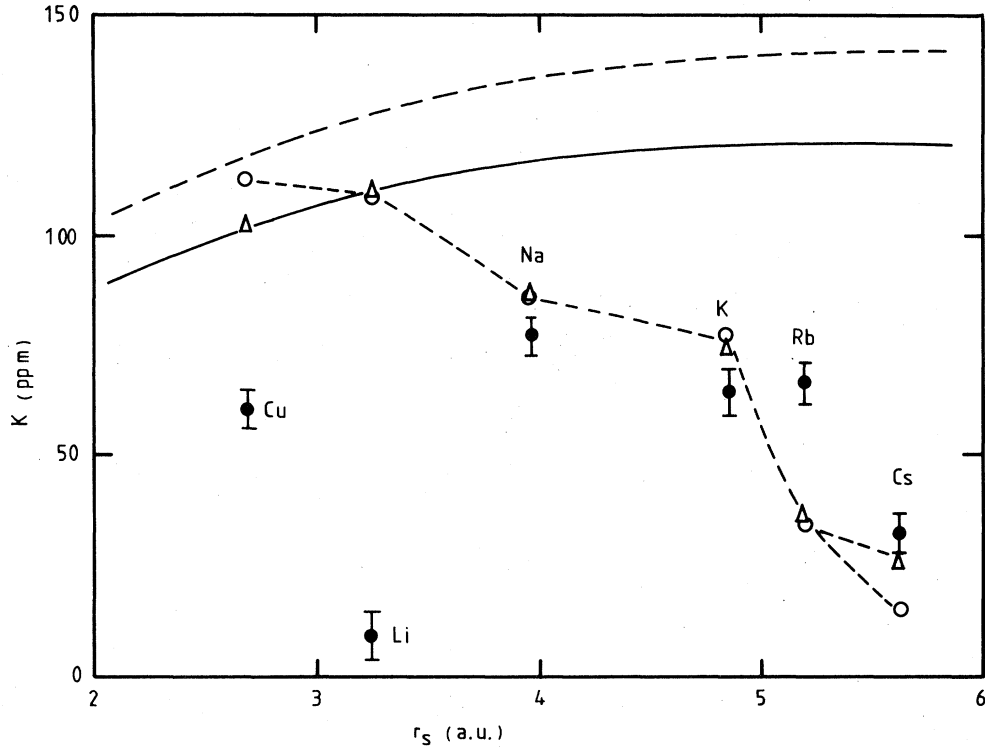


FIG. 1. Muon Knight shift in monovalent metals. The black dots are the experimental results from Ref. 3. The open circles and triangles are the calculated Knight shifts for the octahedral and tetrahedral interstitial sites, respectively. The solid line shows the jellium result, and the dashed line is the jellium result without the diamagnetic shielding.

potential parameter r_c is illustrated in Fig. 3. Both in Cu and in Mg the increase of the core radius decreases the Knight shift fairly rapidly. However, a large increase in r_c (~ 0.5 a.u.) in both metals is needed for bringing the theoretical results in perfect agreement with the experimental ones. One might expect that a larger core radius means a weaker pseudopotential, and the effect of the spherical-solid potential would be smaller. However, the spherical-solid potential $V_{ss}(r)$ results by replacing the electrostatic potential due to the homogeneous positive background of the jellium by unscreened pseudopotentials. The value at the center of the interstitial site is

$$V_{ss}(0) = -\frac{Z^{2/3}\alpha_z}{r_s} - \frac{3r_c^2}{2r_s^3}, \quad (8)$$

where α_z is the relevant Madelung constant,¹⁶ different for different sites, and the zero level is chosen so that $V_{ss}(\infty) = 0$. The difference in $V_{ss}(0)$ between different interstitial sites comes only through the first term, which is totally independent of the pseudopotential, indicating that the spherical-solid potential is never weak, and it has a large effect on the Knight shift in all simple metals.

Owing to the full self-consistency the present calculation includes both the core and Fermi-surface contributions to the contact hyperfine field. Figure 4 shows the contact electron density at the muon in the tetrahedral site in Cs as a function of the electron wave vector. The results are shown for the paramagnetic jellium model and for the spherical-solid model with a polarization

$$(n_0^\uparrow - n_0^\downarrow)/(n_0^\uparrow + n_0^\downarrow) = 0.1.$$

The spin enhancement $\rho_s(\vec{r})$ is proportional to the external magnetic field up to much higher polarizations.⁵ In Fig. 4 the bound states are shown as δ peaks, the height of which gives the corresponding electron density. There are three contributions to the contact spin density: (i) the positive Fermi-surface contribution coming from the repopulation of the one-electron states [this gives the conventional approximation $\rho_s(0) \sim \langle |\psi_F(0)|^2 \rangle$], (ii) the negative core contribution from the bound states, and (iii) a positive contribution coming from the changes in the wave functions of the conduction band below the Fermi level. In the case of Cs all these contributions are of the same order, showing the importance of self-consistency in the calculation. In the spherical-

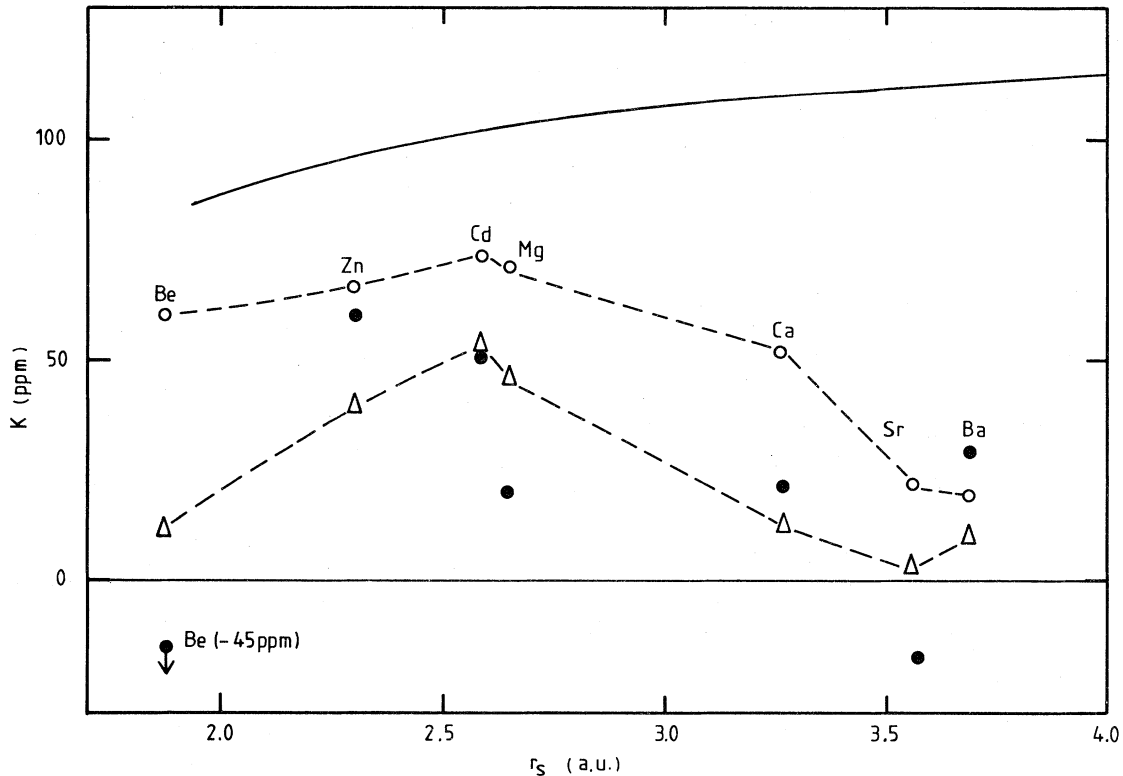


FIG. 2. Muon Knight shift in divalent metals. The black dots are the experimental results from Ref. 3. The open circles and triangles are the calculated Knight shifts for the octahedral and tetrahedral interstitial sites, respectively. The solid line shows the jellium result.

solid model the conduction-electron contribution to the contact electron density is smaller than in the jellium model, whereas the negative core contribution is larger. This explains the large difference in the Knight shift of these two models, although the

total electron density at the muon is almost the same.

The diamagnetic shielding calculated from Eq. (6) contributes to the Knight shift in the jellium model from -15 to 20 ppm as seen from Fig. 1, where the results with and without the diamagnetic shielding are plotted. In the spherical-solid model the diamagnetic contribution is slightly smaller for divalent metals varying from -10 to -15 ppm, whereas for monovalent alkali metals it is essentially the same as in the jellium model.

B. Lattice relaxation around the muon

An experimental estimate²⁵ of the lattice relaxation around an interstitial muon has been made only in Cu where the outward shift of the nearest-neighbor distance in the octahedral site is estimated to be 5%. Keeping the other atomic positions fixed, the 5% relaxation in the nearest-neighbor distance increases the Knight shift of the spherical-solid model by about 10% for Cu, which does not improve the result compared to the experimental Knight shift. For divalent Mg the effect of the lattice relaxation is as small; the Knight shift increases linearly with the nearest-neighbor distance, and 1%

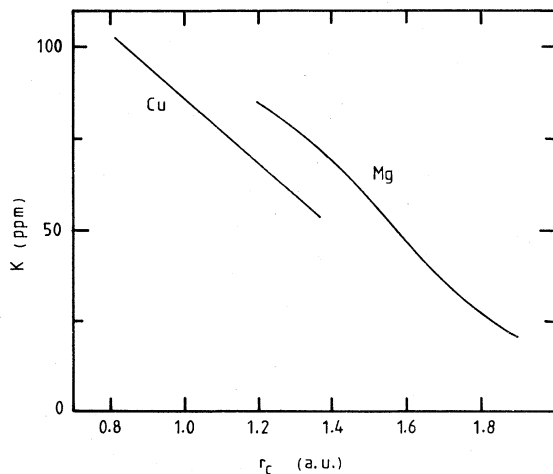


FIG. 3. Dependence of the muon Knight shift on the pseudopotential parameter r_c in Cu and Mg.

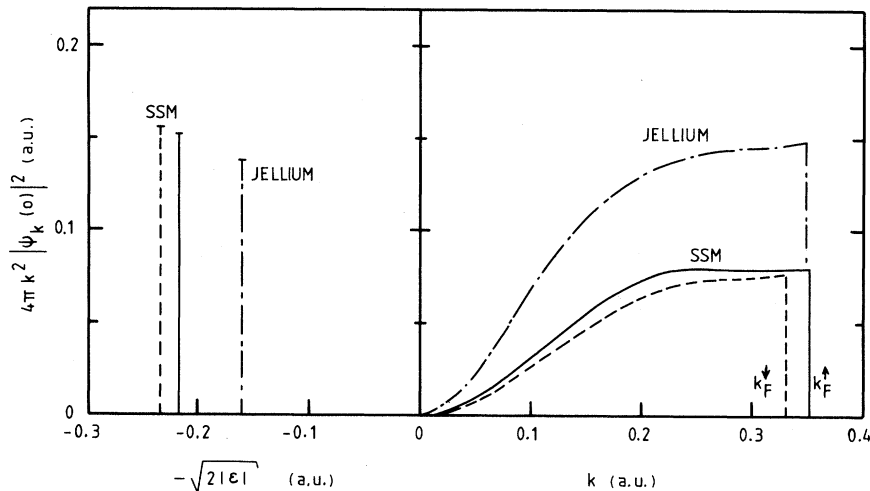


FIG. 4. Partial-wave decomposition of the electron density at the tetrahedral muon site in Cs. The left-hand side shows the bound-state contribution and the right-hand side the conduction-electron contribution to the total electron density. The solid and dashed lines are results of the spherical-solid model for spin-up and spin-down electrons, respectively $[(n_0^\uparrow - n_0^\downarrow)/(n_0^\uparrow + n_0^\downarrow) = 0.1]$. The dotted-dashed line is the spin-up (or spin-down) electron density for the nonpolarized jellium model.

dilatation corresponds to a 1-ppm increase in K . A theoretical estimate for the lattice relaxation around the muon has been made in the case of Al,²⁶ where the result is 2.4%, and it is expected that it is of the same order also for other simple metals. Thus, in general, the effect of the lattice relaxation on the muon Knight shift in simple metals is small, only a few ppm.

C. Effect of the muon zero-point motion

The small difference in the muon Knight shift at different lattice sites in alkali metals suggests that also the effect of the muon zero-point motion in these monovalent bcc metals is very small. The effect of the muon zero-point motion was studied in the case of divalent Mg. Figure 5 shows the adiabatic Knight shift at the muon site when it is displaced from the center of the octahedral site. Displacement to all directions increases the Knight shift. If the muon is assumed to have a Gaussian distribution with a width of 1 a.u., the zero-point motion gives about 10% increase to the Knight shift [calculated from Eq. (7)]. The larger mass of hydrogen would lead to a narrower probability distribution and to a smaller Knight shift. However, the resulting isotope effect would be very small (< 10 ppm). Opposite to the magnetic materials,¹⁷⁻¹⁹ where the zero-point motion has a large effect on the muon hyperfine field, the muon Knight shift in simple metals seems to be fairly independent of the width of the muon distribution.

D. Systematics of the muon Knight shift

For a given valency of the host metal the muon Knight shift shows a systematic behavior as a function of r_s . This is well reproduced by the spherical-solid model and can be understood as follows. The core radius of the pseudopotential r_c increases systematically with the Wigner-Seitz radius of the metal. For alkali metals, e.g., a good approximation for all r_s 's in Table I is

$$r_c = -1.25 + 0.75r_s. \quad (9)$$

With this approximation the Knight shift would

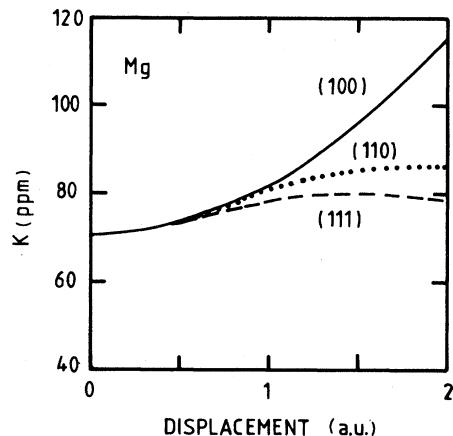


FIG. 5. Muon Knight shift at the octahedral interstitial site in Mg as a function of the muon displacement from the center of the octahedral site along the three main crystallographic directions.

TABLE I. Parameters used in the calculations.

Metal	Lattice structure	Z	r_s (a.u.)	r_c (a.u.)
Cu	fcc	1	2.67	0.81
Li	bcc	1	3.25	1.06
Na	bcc	1	3.93	1.67
K	bcc	1	4.86	2.14
Rb	bcc	1	5.20	2.61
Cs	bcc	1	5.63	2.93
Be	fcc ^a	2	1.88	1.06
Zn	fcc ^a	2	2.31	1.27
Cd	fcc ^a	2	2.59	1.25
Mg	fcc ^a	2	2.65	1.39
Ca	fcc	2	3.27	1.91
Sr	fcc	2	3.56	2.13
Ba	bcc	2	3.69	2.55
Al	fcc	3	2.07	1.12
Pb	fcc	4	2.30	1.12

^afcc structure was assumed for hcp metals.

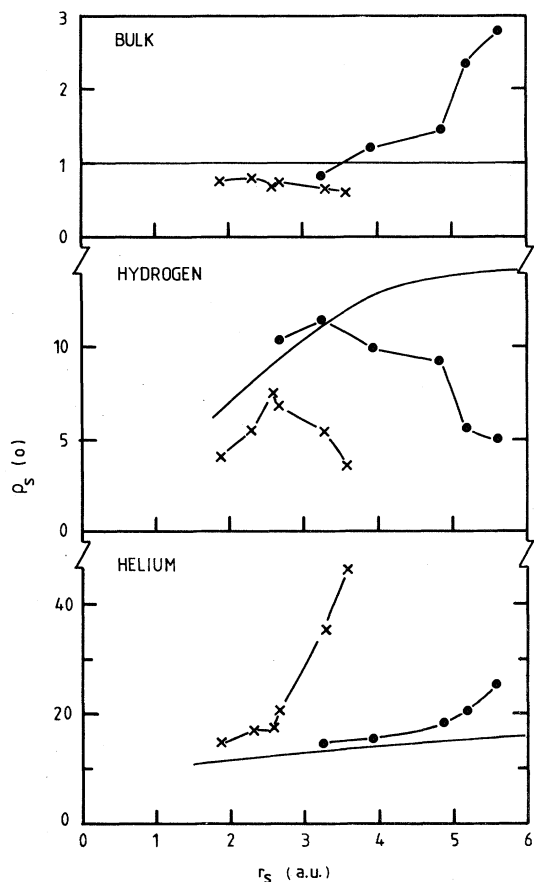


FIG. 6. Spin-density enhancement as a function of the electron-density parameter r_s for the bulk metal, hydrogen impurity, and helium impurity. The solid lines are the jellium results. The black dots and the crosses are the results of the spherical-solid model for tetrahedral interstitial sites in monovalent bcc metals (dots) and for octahedral interstitial sites in divalent fcc metals (crosses).

depend only on r_s . This explains the systematic behavior as a function of r_s seen in Figs. 1 and 2.

A similar systematical behavior of the hyperfine field results also for other impurities and for the host metal. In Fig. 6 the spin-density enhancement $\rho_s(0)$ at the center of the interstitial site is shown for

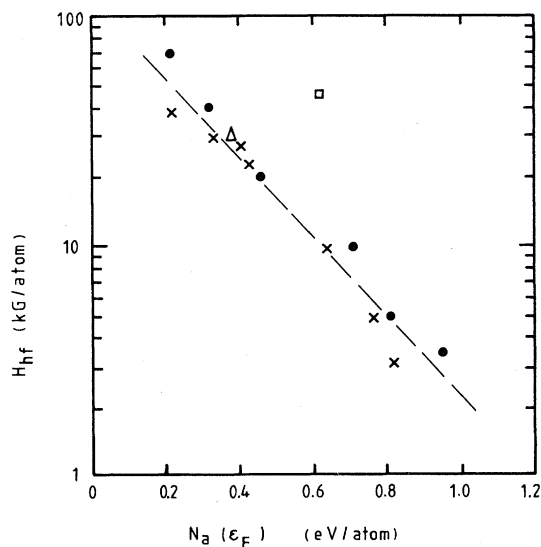


FIG. 7. Calculated hyperfine field at the muon site per host atom, $H_{hf} = (8\pi/3)[n^+(\vec{r}_\mu) - n^-(\vec{r}_\mu)]/\Omega$, as a function of the density of states (per atom) at the Fermi level. The metals from left to right are Cu, Li, Na, K, Rb, Cs (black dots), Be, Zn, Cd, Mg, Ca, Sr, Ba (crosses), Al (triangle), and Pb (square). The dashed line shows the approximate linear relationship. For bcc metals the muon site is the tetrahedral and for other metals the octahedral interstitial site.

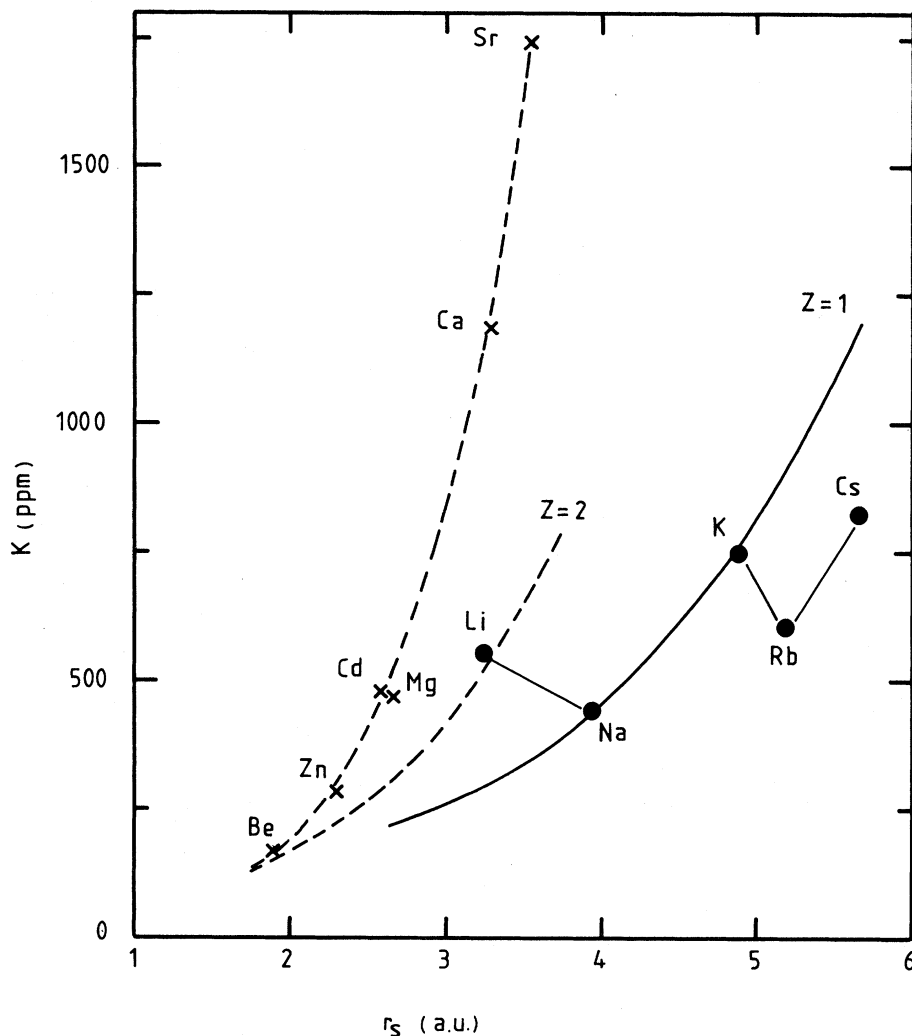


FIG. 8. Muon Knight shift at lattice vacancies as a function of the electron-density parameter of the host metal. The results of the spherical-solid model are shown as black dots and crosses. The solid and dashed lines show the results of the jellium model for monovalent ($Z=1$) and divalent ($Z=2$) metals, respectively.

the bulk metal without impurity, for a positive muon, and for a helium atom. Results are shown for the tetrahedral interstitial site of all monovalent bcc metals and for the octahedral site of divalent fcc metals. In all cases the spin enhancement depends systematically on r_s , but the departure from the jellium result is qualitatively different for different impurities. For muon (or hydrogen) the spherical-solid model gives smaller Knight shifts than the jellium model, whereas for helium the result is the opposite. The response of the impurity Knight shift to the spherical-solid potential depends sensitively on the electronic structure of the impurity. In the ferromagnetic materials, where the lattice potential is spin dependent, this leads to the well-known systematic dependence of the impurity hyperfine field

on the atomic number of the impurity.^{10,27}

Recently, Schenck has found experimentally a linear relationship between the logarithm of the muon hyperfine field per atom and the molar electronic specific heat.³ In simple metals the electronic specific heat can be related to the density of states at the Fermi level. In Fig. 7 we show the calculated hyperfine field per atom as a function of the density of states of the homogeneous electron gas. The logarithm of the hyperfine field is indeed apparently a linear function of the (atomic) density of states. However, this is a specific feature of the hyperfine field at the muon site. From the results shown in Fig. 6 it is obvious that this kind of relationship does not exist for the hyperfine field in the bulk metal or at other impurities.

E. Muon Knight shift at lattice vacancies

The muon Knight shift at the center of a lattice vacancy was calculated both in the jellium model and in the spherical-solid model. The results for alkali metals and divalent fcc metals are shown in Fig. 8. Inside the vacancy the muon Knight shift in all simple metals is several hundred ppm larger than in the interstitial site. As already pointed out earlier¹⁶ this difference should be clearly measurable if a considerable amount of muons would be trapped by vacancies. So far no Knight-shift measurements for muons at lattice vacancies have been done, but the depolarization measurements in quenched aluminium have given evidence of muon trapping in vacancies in aluminium.²⁸ The theoretical prediction for the muon Knight shift in an aluminium vacancy is 467 ppm in the spherical-solid model and 248 ppm in the jellium model.

IV. CONCLUSIONS

In simple metals the impurities are very effectively screened by the conduction electrons and the total electron-density profile of the screening cloud, created by the strong $1/r$ potential, is affected very little by the periodic lattice potential. The spin-density enhancement, on the other hand, is caused by the much weaker exchange-correlation potential. Thus

in calculating the spin density around the impurity the correct variation of the electrostatic lattice potential is essential and has to be included. The spherical average of simple pseudopotentials gives a good local approximation for the true lattice potential, and the resulting muon Knight shifts are in good agreement with the experimental results. The spherical-solid model also explains the observed systematics that for a given valency of the host metal the muon Knight shift is a smooth function of the electron density of the host. A similar systematics is predicted for other impurities in simple metals.

The effects of the lattice relaxation around the muon and the muon zero-point motion have been estimated to be only about 10 ppm or smaller. This also suggests a very small isotope effect between the muon and hydrogen Knight shifts in simple metals. The Knight shifts for muons trapped at lattice vacancies are predicted to be much larger than those for the interstitial muons, suggesting that the Knight-shift measurements can be used for studying muon trapping by defects.

ACKNOWLEDGMENTS

The author would like to thank A. Hintermann, P. F. Meier, and A. Schenck for many useful discussions.

-
- ¹D. P. Hutchinson, J. Menes, G. Shapiro, and A. M. Patlach, *Phys. Rev.* **131**, 1351 (1963).
²M. Camani, F. N. Gyax, W. Rueegg, A. Schenck, and H. Schilling, *Phys. Rev. Lett.* **42**, 679 (1979).
³A. Schenck, *Hyperfine Interact.* **8**, 445 (1981); *Helv. Phys. Acta* (in press).
⁴K. S. Petzinger and R. Munjal, *Phys. Rev. B* **15**, 1560 (1977).
⁵P. Jena, K. S. Singwi, and R. M. Nieminen, *Phys. Rev. B* **17**, 301 (1978).
⁶E. Zaremba and D. Zobin, *Phys. Rev. B* **22**, 5490 (1980).
⁷J. Keller, *Hyperfine Interact.* **6**, 15 (1979).
⁸A. Hintermann, A. M. Stoneham, and A. H. Harker, *Hyperfine Interact.* **8**, 475 (1981).
⁹J. Keller, M. Castro, C. Amador, and E. Orgaz, *Hyperfine Interact.* **8**, 487 (1981).
¹⁰H. Katayama-Yoshida, K. Terakura, and J. Kanamori, *J. Phys. Soc. Jpn.* **48**, 1504 (1980); **49**, 972 (1980).
¹¹O. Jepsen, R. M. Nieminen, and J. Madsen, *Solid State Commun.* **34**, 575 (1980).
¹²J. Arponen and E. Pajanne, *Ann. Phys. (N.Y.)* **121**, 343 (1979).
¹³E. Zaremba and D. Zobin, *Phys. Rev. Lett.* **44**, 175 (1980).
¹⁴M. Manninen and P. Jena, *J. Phys. F* **10**, 1567 (1980).
¹⁵C. O. Almladh and U. von Barth, *Phys. Rev. B* **13**, 3307 (1976).
¹⁶M. Manninen and R. M. Nieminen, *J. Phys. F* **2**, 1333 (1979).
¹⁷J. Rath, M. Manninen, P. Jena, and C. Wang, *Solid State Commun.* **31**, 1003 (1979).
¹⁸S. Estreicher, A. B. Denison, and P. F. Meier, *Hyperfine Interact.* **8**, 601 (1981).
¹⁹M. Manninen and R. M. Nieminen, *J. Phys. F* **11**, 1213 (1981).
²⁰M. J. Puska, R. M. Nieminen, and M. Manninen, *Phys. Rev. B* **24**, 3037 (1981).
²¹N. W. Ashcroft and D. C. Langreth, *Phys. Rev.* **155**, 682 (1967).
²²N. W. Ashcroft and D. C. Langreth, *Phys. Rev.* **159**, 500 (1967).
²³W. M. Shuy and G. D. Gaspari, *Phys. Rev.* **170**, 687 (1968).
²⁴S. P. Singh, *Phys. Rev. B* **2**, 3313 (1974).
²⁵M. Camani, F. N. Gyax, W. Rueegg, A. Schenck, and H. Schilling, *Phys. Rev. Lett.* **39**, 836 (1977).
²⁶F. Perrot and M. Rasolt, *Phys. Rev. B* **23**, 6534 (1981).
²⁷M. Manninen and P. Jena, *Phys. Rev. B* **22**, 2411 (1980).
²⁸J. A. Brown, R. H. Heffner, M. Leon, M. E. Schillaci, D. W. Cooke, and W. B. Gauster, *Phys. Rev. Lett.* **43**, 1513 (1979).